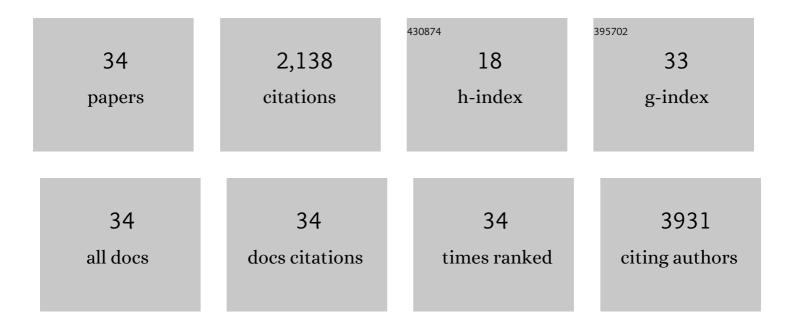
## Kentaro Kuratani

List of Publications by Year in descending order

Source: https://exaly.com/author-pdf/1651037/publications.pdf Version: 2024-02-01



#	Article	IF	CITATIONS
1	From Metal–Organic Framework to Nanoporous Carbon: Toward a Very High Surface Area and Hydrogen Uptake. Journal of the American Chemical Society, 2011, 133, 11854-11857.	13.7	1,071
2	All-Solid-State Battery Electrode Sheets Prepared by a Slurry Coating Process. Journal of the Electrochemical Society, 2017, 164, A2474-A2478.	2.9	125
3	Indigo carmine: An organic crystal as a positive-electrode material for rechargeable sodium batteries. Scientific Reports, 2014, 4, 3650.	3.3	109
4	Na-ion capacitor using sodium pre-doped hard carbon and activated carbon. Electrochimica Acta, 2012, 76, 320-325.	5.2	104
5	Conductivity, viscosity and density of MClO4 (MÂ=ÂLi and Na) dissolved in propylene carbonate and γ-butyrolactone at high concentrations. Journal of Power Sources, 2013, 223, 175-182.	7.8	80
6	Converting rice husk activated carbon into active material for capacitor using three-dimensional porous current collector. Journal of Power Sources, 2011, 196, 10788-10790.	7.8	56
7	Morphological Effect on Reaction Distribution Influenced by Binder Materials in Composite Electrodes for Sheet-type All-Solid-State Lithium-Ion Batteries with the Sulfide-based Solid Electrolyte. Journal of Physical Chemistry C, 2019, 123, 3292-3298.	3.1	53
8	Dry coating of active material particles with sulfide solid electrolytes for an all-solid-state lithium battery. Journal of Power Sources, 2020, 448, 227579.	7.8	50
9	Hydrogen production via steam reforming of ethyl alcohol over nano-structured indium oxide catalysts. Journal of Power Sources, 2008, 179, 566-570.	7.8	48
10	Sulfone-Based Electrolyte Solutions for Rechargeable Magnesium Batteries Using 2,5-Dimethoxy-1,4-benzoquinone Positive Electrode. Journal of the Electrochemical Society, 2014, 161, A1315-A1320.	2.9	47
11	Manganese Oxide Nanorod with 2 × 4 Tunnel Structure: Synthesis and Electrochemical Properties. Crystal Growth and Design, 2007, 7, 1375-1377.	3.0	45
12	Influence of the mesoporous structure on capacitance of the RuO2 electrode. Journal of Power Sources, 2009, 189, 1284-1291.	7.8	41
13	Novel Fabrication of High-Quality ZrO2 Ceramic Thin Films from Aqueous Solution. Journal of the American Ceramic Society, 2005, 88, 2923-2927.	3.8	30
14	Irreversible structural change of a spinel Li4Ti5O12 particle via Na insertion-extraction cycles of a sodium-ion battery. Electrochimica Acta, 2014, 148, 175-179.	5.2	30
15	Controlling of Dispersion State of Particles in Slurry and Electrochemical Properties of Electrodes. Journal of the Electrochemical Society, 2019, 166, A501-A506.	2.9	30
16	Synthesis and luminescence property of Eu3+/ZrO2 thin film by the liquid phase deposition method. Journal of Alloys and Compounds, 2006, 408-412, 711-716.	5.5	28
17	Binderless fabrication of amorphous RuO2 electrode for electrochemical capacitor using spark plasma sintering technique. Journal of Power Sources, 2009, 191, 684-687.	7.8	21
18	A Reversible Rocksalt to Amorphous Phase Transition Involving Anion Redox. Scientific Reports, 2018, 8, 15086.	3.3	21

Kentaro Kuratani

#	Article	IF	CITATIONS
19	Aqueous solution-based synthesis of rare earth-doped metal oxide thin films. Thin Solid Films, 2004, 460, 83-86.	1.8	18
20	Influence of the preparation methods on the electrochemical properties and structural changes of alpha-sodium iron oxide as a positive electrode material for rechargeable sodium batteries. Electrochimica Acta, 2015, 182, 871-877.	5.2	14
21	Transport Phenomena of Nonaqueous Electrolyte Solutions at High Concentrations: A Comparison between the Li- and Na-Systems. Journal of the Electrochemical Society, 2016, 163, H417-H425.	2.9	14
22	A systematic study on structure, ionic conductivity, and air-stability of xLi4SnS4·(1â^'x)Li3PS4 solid electrolytes. Ceramics International, 2021, 47, 28377-28383.	4.8	14
23	Elucidation of Capacity Degradation for Graphite in Sulfide-Based All-Solid-State Lithium Batteries: A Void Formation Mechanism. ACS Applied Energy Materials, 2020, 3, 5472-5478.	5.1	13
24	Capacitive behavior of amorphous and crystalline RuO2 composite electrode fabricated by spark plasma sintering technique. Journal of Power Sources, 2011, 196, 7878-7881.	7.8	12
25	Rheological interpretation of the structural change of LiB cathode slurry during the preparation process. Jcis Open, 2022, 5, 100038.	3.2	12
26	Design of a Sodium-ion Cell with a Carbon-free Li <sub>4</sub> Ti <sub>5</sub> O <sub>12</sub> Negative Electrode. Electrochemistry, 2015, 83, 989-992.	1.4	11
27	Cubic Rocksalt Li <sub>2</sub> SnS <sub>3</sub> and a Solid Solution with Li <sub>3</sub> NbS <sub>4</sub> Prepared by Mechanochemical Synthesis. Electrochemistry, 2017, 85, 580-584.	1.4	11
28	One-compartment electrochemical H2 generator from borohydride. Journal of Power Sources, 2010, 195, 1107-1111.	7.8	10
29	Monte-Carlo Simulation of the Ionic Transport of Electrolyte Solutions at High Concentrations Based on the Pseudo-Lattice Model. Journal of the Electrochemical Society, 2016, 163, H576-H583.	2.9	6
30	Mechanochemical synthesis of air-stable hexagonal Li <sub>4</sub> SnS <sub>4</sub> -based solid electrolytes containing Lil and Li <sub>3</sub> PS <sub>4</sub> . RSC Advances, 2021, 11, 38880-38888.	3.6	6
31	A Monte-Carlo simulation of ionic conductivity and viscosity of highly concentrated electrolytes based on a pseudo-lattice model. Journal of Chemical Physics, 2017, 147, 034904.	3.0	5
32	Preparation of Highly Oriented Porous LiCoO2 Crystal Films via Li-Vapor Crystal Growth Method. Crystal Growth and Design, 2019, 19, 150-156.	3.0	2
33	Anion Redox in an Amorphous Titanium Polysulfide. ACS Applied Materials & Interfaces, 2022, 14, 33191-33199.	8.0	1
34	Identification of Soluble Degradation Products in Lithium–Sulfur and Lithium-Metal Sulfide Batteries. Separations, 2022, 9, 57.	2.4	0